Brian Kilgore
U.S. Geological Survey,
Earthquake Science Center,
Menlo Park, CA 94025
e-mail: bkilgore@usgs.gov

Julian Lozos
Department of Earth Sciences,
University of California,
Riverside, CA 92521
e-mail: jlozo001@ucr.edu

Nick Beeler
U.S. Geological Survey,
Earthquake Science Center,
Menlo Park, CA 94025;
U.S. Geological Survey,
Cascades Observatory,
Vancouver, WA 98683
e-mail: nbeeler@usgs.gov

David Oglesby
Department of Earth Sciences,
University of California,
Riverside, CA 92521
e-mail: david.oglesby@ucr.edu

Laboratory Observations of Fault Strength in Response to Changes in Normal Stress

Changes in fault normal stress can either inhibit or promote rupture propagation, depending on the fault geometry and on how fault shear strength varies in response to the normal stress change. A better understanding of this dependence will lead to improved earthquake simulation techniques, and ultimately, improved earthquake hazard mitigation efforts. We present the results of new laboratory experiments investigating the effects of step changes in fault normal stress on the fault shear strength during sliding, using bare Westerly granite samples, with roughened sliding surfaces, in a double direct shear apparatus. Previous experimental studies examining the shear strength following a step change in the normal stress produce contradictory results: a set of double direct shear experiments indicates that the shear strength of a fault responds immediately, and then is followed by a prolonged slip-dependent response, while a set of shock loading experiments indicates that there is no immediate component, and the response is purely gradual and slip-dependent. In our new, high-resolution experiments, we observe that the acoustic transmissivity and dilatancy of simulated faults in our tests respond immediately to changes in the normal stress, consistent with the interpretations of previous investigations, and verify an immediate increase in the area of contact between the roughened sliding surfaces as normal stress increases. However, the shear strength of the fault does ***not*** *immediately increase, indicating that the new area of contact between the rough fault surfaces does not appear preloaded with any shear resistance or strength. Additional slip is required for the fault to achieve a new shear strength appropriate for its new loading conditions, consistent with previous observations made during shock loading.* [DOI: 10.1115/1.4005883]

1 Introduction

Due to symmetry in geometry and materials, slip on a vertical fault in a laterally homogeneous material induces a change in shear stress on the fault, but not a change in normal stress. However, slip on nonplanar faults or on faults in heterogeneous materials can also induce changes in normal stress, leading to a complex time history of fault friction (e.g., Harris et al., [1], Andrews and Ben-Zion [2], Bouchon and Streiff [3], and Harris and Day [4]). Rupture propagation at fault bends, step-overs, and branch points are prime examples of geometrical features which lead to changes in normal stress that may affect the rupture extent and speed; numerical models have implied that normal stress changes may cause such geometrical discontinuities to act either as barriers to rupture or aid in rupture propagation (Harris and Day [5], Kame et al. [6], Bhat et al. [7], Duan and Oglesby [8], and Oglesby [9]). Consistent with these numerical models, observations (Wesnousky [10,11]) imply that around two thirds of earthquake ruptures terminate at zones of geometrical discontinuity, but that many such zones still support through-going rupture. Additionally, a dynamic increase or decrease of normal stress on bimaterial faults may impose preferred rupture directivity (e.g., Weertman [12]), although application of this effect to the earth is controversial (Harris and Day [13]). Understanding what conditions lead to arrest rather than continued propagation through zones of geometric and material complexity requires an understanding of the dependence of friction on normal stress.

How changing normal stress affects propagating ruptures obviously depends on the sensitivity of the fault strength to normal stress. For example, simple friction theory (Bowden and Tabor [14]) suggests that fault shear resistance τ is proportional to normal stress s_n through a friction coefficient μ, $\tau = \mu\sigma_n$. Under this assumption, regions of a fault in which the approaching rupture imposes increasing normal stress (clamping), for example, at a compressive fault branch, are unfavorable for further slip, and regions where the normal stress is reduced by the approaching rupture (unclamping) are more favorable for continued propagation. Likewise, slipping regions that experience increased normal stress will experience less slip than regions that are unclamped. Unfortunately, existing laboratory measurements of the sensitivity of fault shear resistance to changing normal stress are not consistent with the simple time-independent friction coefficient previously described. Furthermore, prior laboratory studies on the effects of normal stress on friction are not consistent with one another, making it unclear as to what behavior is appropriate for use in earthquake models.

The most widely cited previous laboratory studies of the normal stress dependence of fault strength on bare rock surfaces are by Hobbs and Brady [15], Olsson [16], and Linker and Dieterich [17], which were all conducted at room temperature. We focus on experiments where the normal stress is rapidly changed while the fault is sliding initially at a constant slip rate (normal stress step tests). Hobbs and Brady [15], Olsson [16], and Linker and Dieterich [17] all conducted normal stress step tests, and while the results are not identical, they do all find that a step increase in the normal stress results in a somewhat complicated response involving at least two stages. For step increases on gabbro, Hobbs and Brady [15] describe an 'instantaneous' increase in shear stress followed by a further approximately exponential time dependent increase. The relative sizes of the instantaneous and slow responses are not described. Olsson [16] conducted normal stress step tests on welded tuff between 1.5 and 4 MPa normal stress and found a two stage response consisting of an 'immediate' component followed by a slow response that is approximately exponential in slip. The immediate response to an increase in normal stress appears as a steep linear increase when shear stress is

Manuscript received July 1, 2011; final manuscript received November 17, 2011; accepted manuscript posted February 6, 2012; published online April 4, 2012. Assoc. Editor: Eric M. Dunham.

plotted versus slip; Olsson's interpretation is that this is a brief sticking of the fault surface induced by the normal stress increase. Generally, the slow response in Olsson's step tests exceeds the immediate response.

The most detailed study is Linker and Dieterich's [17], conducted on Westerly granite in a biaxial press at normal stresses between 5 and 7 MPa. The response to a step change in normal stress follows three stages in these experiments. Despite the complicated response, these experiments build on the previous studies by Hobbs and Brady [15] and Olsson [16], and provide the primary cited dataset on the normal stress sensitivity of rock friction and the foremost constitutive model for rock friction under variable normal stress. As shown in Fig. 1 (taken from Linker and Dieterich [17]), the first stage in the response to a step increase in normal stress is an instantaneous increase in shear stress. This instantaneous response is marked on each of the plots in Fig. 1 by an open circle. The instantaneous response is a machine effect; that is, an unwanted elastic coupling of shear stress to normal stress. This is thought to result from the slight misalignment of the loading frame or differential Poisson expansion across the fault surface as the fault normal stress is changed. It is likely that the instantaneous response reported by Hobbs and Brady [15] has a similar origin. The second stage is an additional increase from the open circle to the solid circle in Fig. 1 that appears to be linear in displacement.

To understand what is occurring during the second stage response in Linker and Dieterich's [17] test, and to understand their interpretation of it, requires consideration of the interaction between the loading system and the fault. Prior to the imposed normal stress change, the fault is sliding at a constant rate, which is the result of displacing the load point at a prescribed rate. There is a small amount of elastic compliance between the load point and the fault. Typically, the compliance is from elastic strain in the loading piston, the rock blocks on either side of the fault, and the frame of the deformation apparatus. The loading system can be characterized with a single elastic element such that the shear stress on the fault is the difference between the controlled displacement δ_L and the displacement of the fault times the elastic stiffness between the control point and the fault

$$\tau = k(\delta_L - \delta) \tag{1}$$

where k is the stiffness as measured between the fault and the load point, δ_L is load point displacement and δ is fault slip. It is this load point displacement δ_L that is plotted as the horizontal axis in Fig. 1.

As the normal stress is increased in Linker and Dieterich's [17] step test, if the fault slip rate immediately decreased to much less than the loading velocity then, as required by Eq. (1), the shear stress would increase linearly with load point displacement, with a slope equal to the load point stiffness. This is Linker and Dieterich's [17] explanation of the second stage in their experiments, and it is Olsson's [16] explanation of the immediate increase in his tests. Linker and Dieterich's [17] physical interpretation is that as the normal stress is rapidly increased, there is an immediate increase in the real contact area on the sliding surface. The increase in contact area makes the fault stronger, causing the fault slip rate to plummet and the measured shear stress to increase linearly with load point displacement. Following the linear loading, the third stage of the response is that the shear stress gradually

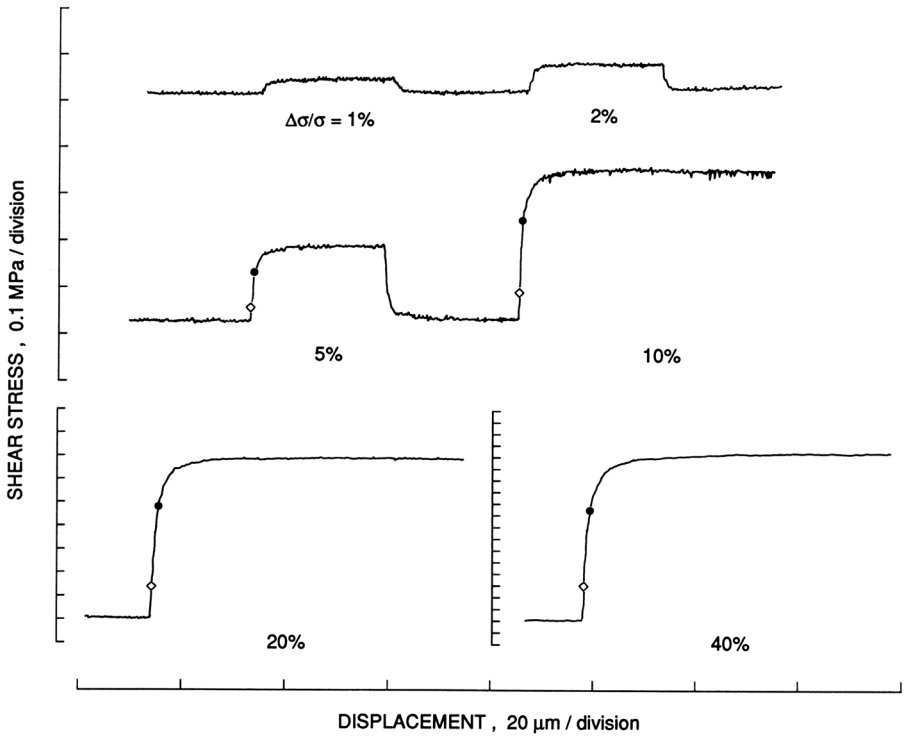

Fig. 1 Effect of changes in normal stress on shear stress for bare granite at room temperature and 5 MPa normal stress from the prior study of Linker and Dieterich [17]. Shear stress versus load point displacement for changes in the normal stresses of 1, 2, 5, 10, 20, and 40% of the ambient value. Note that the 40% change is shown at a compressed vertical scale compared to the other tests. Linker and Dieterich [17] interpret the response to have 3 components. First, there is an instantaneous change marked by the open circle. This is a machine effect due to misalignment of the loading frame or Poisson expansion of the fault surface as the fault normal stress is changed. Next, there is an immediate change from the open circle to the solid circle; this is interpreted as an immediate increase in contact area due to the increased normal stress. Subsequently, there is a further prolonged increase in shear resistance with displacement.

increases asymptotically, approximately exponentially with accumulated slip, to a new steady state level. Linker and Dieterich [17] find that the third stage slow response is smaller than the immediate response.

Hong and Marone [18] conducted similar normal stress step tests on 3 mm thick quartz gouge layers and quartz-smectite mixtures and inferred the same three stage response, consisting of instantaneous, immediate, and slow components, as in Linker and Dieterich [17]; data shown in their paper have been corrected for the instantaneous first stage. Additionally, in agreement with Linker and Dieterich [17], they find that the slow response is smaller than the immediate.

In contrast to Linker and Dieterich [17] and Hong and Marone [18], Prakash [19] presented results from laboratory experiments showing that the shear stress on a sliding interface does not respond immediately to step changes in the applied normal stress (Fig. 2), but gradually evolves to a new steady state level, apparently as a function of accumulated slip. In other words, the entire response of shear stress to a rapid normal stress change is slow. Prakash [19] used bimaterial interfaces consisting of 4340 VAR steel, or 6AI-4V titanium alloy samples, and tungsten carbide targets. To eliminate the problematic effects of a conventional loading frame testing apparatus, e.g., machine stiffness and response rate, Prakash [19] employs high interface slip velocities (1 to 30 m/s), high normal stress (500 to 3000 MPa), and plate-impact pressure-shear techniques in his work. By eliminating the conventional loading frame test apparatus and using holographic methods to measure the normal and transverse particle velocities on the rear surface of the target sample associated with the impact, Prakash [19] measures the intrinsic properties of the frictional response of the simulated fault as the normal stress is changed, and calculates the normal stress and shear stress projected onto the sliding surface in his tests.

The different experimental responses of Linker and Dieterich [17] and Prakash [19] imply very different sensitivities of the sliding rate to normal stress change. For example, for normal stress decreases, Linker and Dieterich [17] suggest that shear resistance decreases immediately in concert with the normal stress, possibly leading to unstable slip, while Prakash's [19] observations suggest that shear resistance does not decrease immediately with decreasing normal stress, implying a more stable response. Rice and colleagues have suggested, on the basis of the rapidity of experimental measurements, shock loading for Prakash [19] versus near quasi-static conditions for Linker and Dieterich [17], that Prakash's [19] observations may be more appropriate for models of dynamic rupture, despite those measurements being on bimaterial interfaces of tungsten carbide and stainless steel or titanium rather than rock (Ranjith and Rice, [20] and Rice et al. [21]).

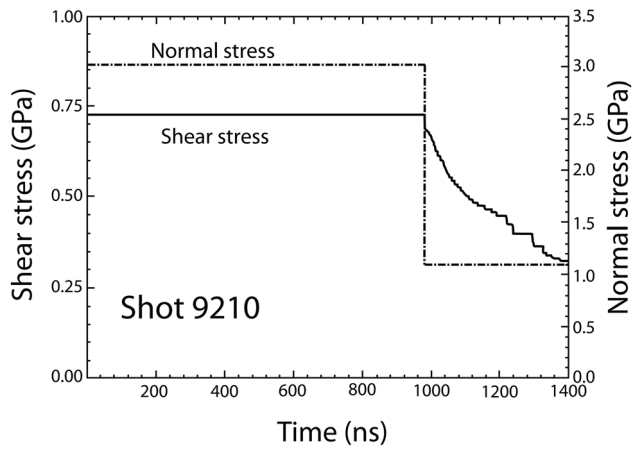

Fig. 2 Response of shear resistance of a bimaterial interface of WC and 4340 structural steel to changes in normal stress at high stress from the prior study of Prakash [19]. Shear (solid line) and normal (dotted-dashed line) stress with time during imposition of a large reduction in normal stress. The normal stress change does not induce a significant immediate change in shear resistance, rather, virtually the entire response is slow.

Rice et al. [21] and Ranjith and Rice [20] also found the Linker and Dieterich [17] formulation problematic when used in models of dynamic fault slip between dissimilar materials. They found that all constitutive equations, including the one proposed by Linker and Dieterich [17], that allow an immediate change in shear resistance accompanying a normal stress change are "ill-posed," This means that shear stress perturbations are unstable and have no solution. If, however, shear resistance evolves with time or displacement following a change in normal stress, such as seen in Prakash's [19] experiments, solutions can be obtained. Thus, resolving the detailed response of the shear resistance to rapid changes in normal stress in faulted rock is a basic need in earthquake physics and dynamic fault mechanics.

In this report, we investigate the discrepancy illustrated by the contrasting results of Linker and Dieterich [17] and Prakash [19]; immediate versus slip-dependent evolution of fault shear stress in response to changes to the normal force applied to the simulated fault. New laboratory experiments have been performed, using the methods and equipment described in Linker and Dieterich [17], to examine how abrupt changes in normal stress affect the strength of a fault. Improved data recording technology and new experimental capabilities allow us to build upon the work of Linker and Dieterich [17]. We document the response of shear stress, fault closure, and the transmissivity of acoustic signals across the simulated fault as the normal stress applied to the simulated fault is varied. We also examine the constitutive relations and physical interpretations of Linker and Dieterich [17] and Prakash [19] in light of the new data presented here.

2 Experimental Procedures

Linker and Dieterich [17] performed three distinct types of experiments: velocity stepping, normal stress stepping, and normal stress pulse tests. In this study, we focus on normal stress stepping tests. We examine how shear stress, fault closure, and the acoustic transmissivity across a simulated fault respond to discrete step changes in the applied normal stress, while initially sliding at steady-state conditions at a constant slip rate. Using the same hydraulically powered double direct shear test apparatus, we use the experimental procedures of Linker and Dieterich [17] as a guide for our work (see Fig. 3). While imposing a load point fault slip rate (V_L) of 1 μm/s, and after sufficient slip has occurred such that the shear stress is constant, we impose normal stress steps up from, and back down to, the baseline normal stress of 5 MPa. The normal stress steps increase in magnitude in increments of 1, 2, 4, 5, 10, 20, and 40% of the baseline 5 MPa normal stress. The duration of the steps up in normal stress is 50 s (50 μm), and the steps are separated by 50 s (50 μm) of slip at the nominal normal stress of 5 MPa. Slip of 50 μm was sufficient for steady-state slip to be achieved during each step.

Several improvements to the test apparatus have been implemented in the time since Linker and Dieterich [17] performed their experiments, which positively impact the results we present here. However, many of the experimental techniques reported by Linker and Dieterich [17] remain as standard test procedures today. For example, the 5 cm $\times$ 5 cm and 5 cm $\times$ 8 cm sliding surfaces of the Westerly granite sample blocks are still prepared by hand lapping those surfaces with #60 silicon carbide abrasive and water on a glass plate. The resultant roughened surfaces were checked to be flat and parallel to a reference surface to within 0.025 mm. In addition, we continue to mount our slip sensor directly to the sample blocks. The stability of fault slip in response to increases in loading rate, and decreases in normal stress, depends on the rate that the fault strength changes with slip and on the stiffness of the loading apparatus. Stiffness is the rate shear stress applied to the fault changes with displacement of the

loading point (Dieterich [22]). Instability results when the rate of strength loss exceeds the loading stiffness. The servo-controlled system loading the fault uses the output of a small capacitive position sensor, mounted on the sample blocks a few millimeters from the fault. The proximity of the slip sensor to the fault minimizes the compliance between the load point and the fault; thus maximizing the stiffness of the loading system. Accordingly, measured 'load point' displacements contain both actual fault slip and a small amount of elastic distortion of the sample spanning the fault, between the slip sensor mounting points. An identical position sensor, mounted on the samples orthogonal to the fault surfaces, measures fault closure throughout the tests.

We employ 16-bit digital data recorders to record the signals generated by the various sensors. Linker and Dieterich [17] relied on an analog X-Y plotter and several strip chart recorders to record their data. The servo-mechanical response of analog data recorders effectively imposed a low pass filter on the recorded sensor signals with a cut-off frequency of about 2 or 3 Hz. All of the data collected in the present study were saved at the rate of 100 pt/s (Hz). Each saved data point represents 10 data points recorded at 1000 Hz, averaged in real time, and then saved on the host computer. This results in an increase in the temporal resolution of our data by at least an order of magnitude compared to the data records available to Linker and Dieterich [17].

The servo-control electronics employed by Linker and Dieterich [17] used standard proportional (P) servo circuits. A proportional servo circuit linearly amplifies the difference between a reference signal, typically computer generated, and a sensor feedback signal, monitoring the force or position that is being controlled, producing an error signal. The error signals drives the servo valves, which control the flow of hydraulic oil into, and out of, the hydraulic cylinders which generate the normal and shear forces in the test apparatus. When using a servo system with only a proportional gain response, a balance among minimizing error, signal drift, and low frequency oscillations, often observed at low error signal gains, competes against an over-sensitive feedback loop at high error signal gains, making the system prone to instability and overshoot. We use proportional–integral-derivative (PID) servo electronics to control the test apparatus in the current experiments. In addition to amplifying the error signal using proportional gain, a PID controller integrates the error signal, essentially summing recent error signals, and determines the derivative of the recent error signal, responding to the rate at which the recent error signal has changed. The response of a PID servo controller is the sum of the proportional, integral, and derivative response to the error signal. When properly tuned, a PID servo system maximizes sensitivity and simultaneously minimizes overshoot, drift, and oscillation errors as the test apparatus compensates for changes to the control signal. We use PID servo electronics to control both the normal stress, and the fault slip position, which improves the stability of the system when the normal stress is stepped up and down. The stability of steps down in normal stress ensured that stable steady-state slip, punctuated by a series of normal stress steps which increase in magnitude during an experiment, is continuous throughout the experiment.

An artifact of the servo system as implemented, however, is a small amount of noise observed in the measured slip records. As the servo system attempts to track a continuously moving reference position signal to produce a constant load point velocity, a small oscillation in the recorded fault position signal is observed. This oscillation of the position signal is small, and usually inconsequential, relative to the scale at which these data are typically examined. However, in these experiments, we examine the data relative to microns of slip data, rather than tens or hundreds of microns of slip data, typically employed for similar laboratory experiments. To avoid the distraction of the analysis of other data relative to noisy observed slip data at these scales, we examine our data relative to the product of the elapsed time $\times$ load point velocity $V_{L,}$ which, in these experiments, is coincidentally equivalent to the elapsed time during the experiment.

We also utilize ultrasonic acoustic sensors in these experiments to infer relative changes in the real area of contact between the

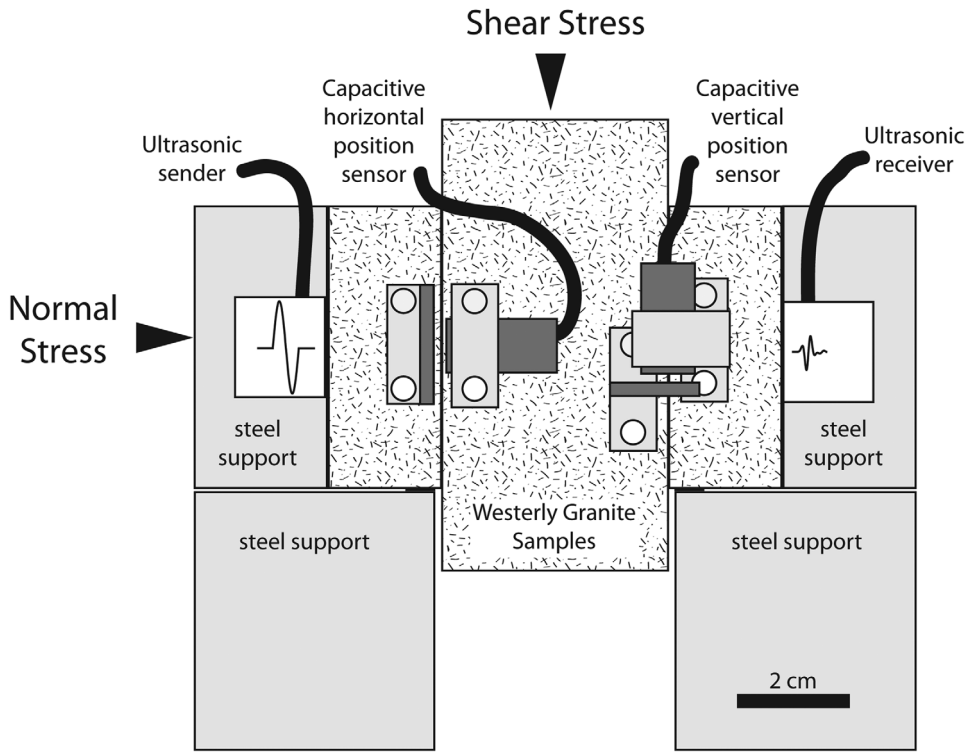

Fig. 3 The biaxial experimental geometry used, consisting of applied shear and normal forces. Instrumentation includes a fault slip sensor, a fault normal displacement sensor, and a pair of acoustic transmitters/receivers.

sliding surfaces of the fault, following the methods developed by Nagata et al. [23,24]. We measure the peak-to-peak amplitude of the received sine wave pulses after they have traversed the sample assembly. A sine wave pulse is produced at the source transducer once every 0.01 s. Each pulse is a 20 V peak-to-peak 1 MHz wave, generated using a Tabor WW2572A waveform generator. The pulse is imposed using a Panametrics V103-RM single element longitudinal wave transducer with a 1 MHz center frequency and, after propagating through the sample assembly, is detected by a second, identical V103-RM transducer. The received signal is amplified and passed through a 300 kHz high pass filter and a 5 MHz low pass filter using a Panametrics 5800 pulser/receiver. The received sine wave pulses are digitized at the rate of 100 MHz with 14-bits of resolution.

3 Results

A representative series of increasing steps at progressively higher normal stress are shown in Figs. 4(*a*) normal stress, 4(*b*) shear stress, 4(*c*) acoustic transmissivity, 4(*d*) horizontal closure, and 4(*e*) observed slip, plotted against the elapsed time (bottom axes) and load point displacement (top axes). As described in the Introduction and Experimental Procedure sections, the fault is loaded in shear by specifying a load point displacement rate V_L. The product of the elapsed time and V_L is the specified load point displacement that is used as a control signal for the servo system, and is also what we plot our data relative to, in order to avoid the distractions of noise in the observed slip record at the micron scale. The axes on all of the plots have been limited to the first two microns or seconds following the step increases in the normal stress. The focus on the first two microns or seconds following normal stress steps, allows the details of the evolution of the shear stress, fault dilation/closure, and the acoustic transmissivity across the fault, to be easily viewed.

Stable steps up in the normal stress between 5 MPa and 7 MPa, were achieved in 0.1 s with less than 0.01 MPa of overshoot. Specific to these tests, even though we do not report data from steps down in normal stress, we are able to conduct stable down steps in normal stress to 5 MPa after steps up to as high as 6 MPa. However, down steps in normal stress were not presented in detail by Linker and Dieterich [17], which is the focus of the comparisons in the present study. Linker and Dieterich [17] assumed that down steps were symmetric to the up-steps, and our data do not dispute this assumption. However, the largest down-steps in normal stress observed in this study, from 7 MPa to 5 MPa, are complicated by instability. The down-steps from all of the normal stresses that are stable are likely associated with large excursions in slip rate, which introduce apparent asymmetry with the up steps, necessitating analysis beyond the scope of this work.

The use of smaller capacitive position sensors to measure fault slip and fault closure allows us to mount those sensors directly onto the samples, within a few millimeters of the fault. Since we measure load point displacement and closure very near the fault, the observed measurements contain only a small component of the elastic displacements within the rock surrounding the fault. A direct result of the shear displacement sensor location is an improved load point stiffness of ~0.75 MPa/μm, versus 0.5 MPa/μm reported by Linker and Dieterich [17].

The fault closure data are obtained directly from a sensor spanning one fault surface, and are not corrected for deformation associated with bulk elastic deformation of the rock between the sensor and target mounting points that arise when normal and shear stress are changed. Corrections due to changes in normal stress are of the order of 0.28 μm/MPa, which is roughly 10% of the immediate closure, and would be of the sense to reduce the amplitude of the measured fault closure. The elastic distortion accompanying changes in shear stress are expected to be on the order of 0.05 μm/MPa, similar in magnitude to the small observed slow response of closure. The correction for this effect would be of the sense to increase the measured closure. Because these corrections are, at present, not well calibrated, and because the closure data are not used quantitatively in the present study, we have not corrected the closure for these elastic effects.

Following the work of Nagata et al. [23], the acoustic transmissivity of the sliding surfaces |T| in this double direct shear geometry is

$$|T| = \sqrt{\frac{A}{A_i}}$$

where A is the measured amplitude of the received sine wave pulse traversing the entire sample assembly, and A_i is the amplitude of an identically sourced sine wave, traversing a single, solid block of Westerly granite that is the same thickness as the sample assembly. The acoustic transmissivity of a fault has been interpreted as a proxy for the area of contact between the roughened fault surfaces (Nagata et al. [23,24]). When combined with the fault closure measurements, these observations provide a continuous record of deformation occurring between the sliding fault surfaces. These measurements clearly show an immediate physical response of the fault surface as the normal stress is changed. The simultaneous closure of the fault surfaces is consistent, indeed necessary, for an increase in the contact area across the rough fault surfaces.

The observed shear stress, however, clearly shows a gradual evolution as the normal stress is changed. Thus, our observed shear stress response to rapid changes in normal stress differs from that of Linker and Dieterich [17] and Hong and Marone [18] in two ways. Our measurements lack the instantaneous coupling of the shear stress to normal stress change (open symbols in Fig. 1) and they also lack the immediate response, which is evident as a linear stage in plots of shear stress versus load point displacement (solid symbols in Fig. 1). To ensure that the slow response components of observed shear stress, acoustic amplitude, and closure that appear as slip dependent effects when plotted versus load point displacement, are not actually time dependent, identical tests were performed with the nominal slip rate as low as 0.1 μm/s and as high as 5 μm/s. Observations from those tests confirmed our initial interpretation that, in all cases, the shear stress on the fault is slow to respond to changes in the normal stress applied to the fault, and that the slow response of shear stress and the slow components of closure and acoustic amplitude can be interpreted as slip- rather than time-dependent.

4 Discussion

Improvements in our experimental capabilities allow us to examine portions of the work previously presented by Linker and Dieterich [17] in more detail, and in the context of the more recent work of Prakash [19]. While these studies reach different conclusions on how the shear strength of a sliding fault responds to changes in the applied normal stress, neither of these datasets is definitive; rather, they are subjective interpretations based, in part, on models. For example, Linker and Dieterich [17] do not strictly observe an immediate increase in fault strength because there is finite compliance in the loading system, nor do they observe a change in contact area. What is observed is a gradual increase in shear resistance that appears to follow the loading stiffness of the machine. Thus, theirs is an interpreted immediate increase in strength and contact area. Another difficulty in making comparisons with Linker and Dieterich [17] is that the evolution distance d_c in their experiments is approximately 1 μm but the plots of the response have a displacement axis length of 80 μm, which is far too coarse to examine the immediate response in detail. The immediate strengthening is well reflected in the constitutive relationships they developed. In the following section, we use predictions from those relationships to compare with our more detailed measurements.

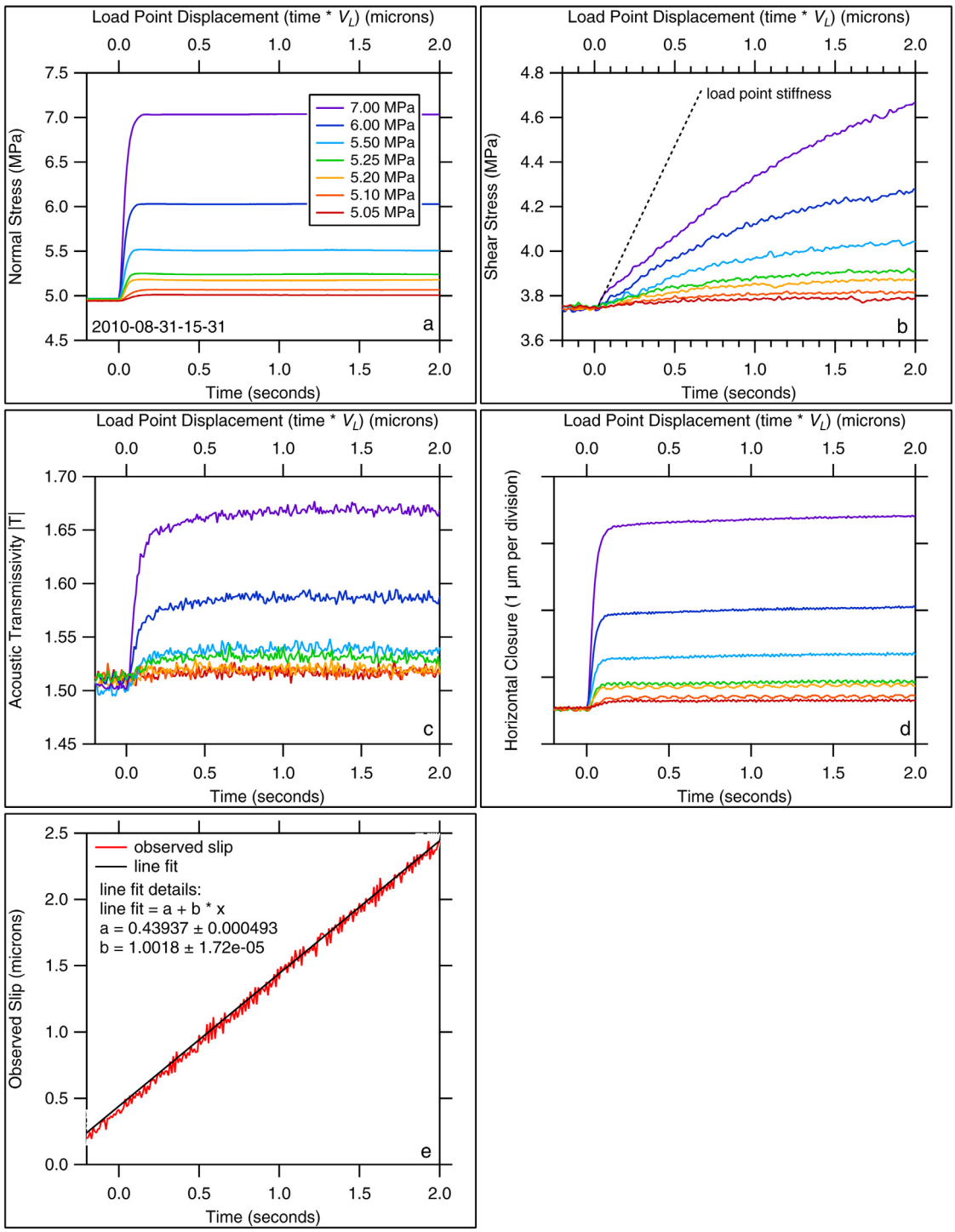

Fig. 4 Representative data showing (*a*) step changes in normal stress, and the subsequent response of (*b*) shear stress, (*c*) acoustic transmissivity, and (*d*) fault closure, responding to the change in fault normal stress, plotted versus load point displacement × load point velocity (1 μm/s). (*b*) A line with slope equal to the estimated stiffness of the loading system ($\sim$0.75 MPa/μm) is shown for reference. (*e*) Observed fault slip during a step up in normal stress (time = 0) from 5 MPa to 7 MPa.

Likewise, Prakash's [19] interpretation of a slip dependent shear strength response is indirect. Slip, slip speed, shear, and normal traction at the sliding interface are not directly measured in these experiments; they are all inferred using elastodynamic theory from velocities measured at the free surface on the back of the tungsten carbide block that makes up the stationary side of the fault. Prakash [19] also developed constitutive relations for the normal stress response. Because our experiments are conducted using entirely different experimental techniques, time scales, and physical conditions, determining consistency with Prakash's [19] observations can only be accomplished by comparing our observations with the predictions of his constitutive relations applied to the conditions of our experiments.

Linker and Dieterich [17] developed the constitutive description of their data using a modification of standard rate and state relations

$$f = f_0 + a\ln(V/V_0) + b\varphi \tag{2a}$$

$$\frac{d\varphi}{dt} = -\frac{V}{d_c}\left[\varphi + ln\left(\frac{V}{V_0}\right)\right] - \frac{\alpha}{b\sigma}\frac{d\sigma}{dt} \tag{2b}$$

where f is friction, the ratio of shear stress to normal stress, f_0 is a first-order constant, a and b are second order constants, V is slip speed, V_0 is a reference slip speed, d_c is a characteristic length scale, σ is normal stress, and α is a constant that controls the predicted response of friction to changes in normal stress. Here, ϕ is a state variable with the physical interpretation of the fractional contact area on the sliding surface that is associated with time dependent creep at asperity contacts. Linker and Dieterich [17] assumed that the steady state coefficient of friction f_{ss}, the state variable ϕ_{ss} at steady-state (equal to $\ln V/V_0$), the critical slip distance d_c, and the empirically determined constitutive parameters a and b, are insensitive to normal stress within the range of the normal stresses they tested. To simulate the effects due to changes in normal stress, they postulated the following: changes in normal stress result in changes in state ϕ, and all state effects resulting from changes in either normal stress or slip rate can be described by a single state variable. The state is defined as a function of V, σ, ϕ, and d_c, and a sudden change in σ results in a sudden change in ϕ that is symmetric with regard to increases versus decreases in σ. They further postulate that following the sudden change in state, with continued sliding, the state returns to its previous value.

A key component to the Linker and Dieterich [17] conceptual model is that a sudden increase in the normal stress causes the real area of contact between the sliding surfaces to immediately increase. If the frictional strength of the fault is proportional to the area of the load-bearing contacts between the sliding fault surfaces, the shear resistance should respond immediately to the change in area, e.g.

$$\tau = sA \tag{3}$$

given by Bowden and Tabor [14], where τ is shear stress or shear resistance, s is the contact yield shear strength, and A is the fractional contact area. Following this immediate increase, the contact area evolves with displacement to a new steady-state value. Thus, their resulting constitutive equations are composed of two contributions: an immediate effect and a delayed effect. For step changes in normal stress at the constant slip rate, such as shown in Fig. 1, the slow change in shear stress logarithmically depends on the size of the normal stress change as

$$\frac{\Delta\tau}{\sigma} = \alpha \ln\frac{\sigma}{\sigma_0} \tag{4}$$

where σ_0 is the starting normal stress (Linker and Dieterich [17]). If these shear stress changes are equated with changes in the steady-state fractional contact area associated with creep at asperity contacts $\Delta\tau/\sigma = b\Delta\phi$, the state changes with normal stress as

$$\phi = \phi_0 + \frac{\alpha}{b}\ln\left(\frac{\sigma}{\sigma_0}\right) \tag{5}$$

Linker and Dieterich [17] assume that at the time of the normal stress change, the fractional contact area is immediately offset by this amount. The state evolves with time, following Eq. (2*b*). To maintain steady-state friction independent of normal stress, the evolution equations are used with the standard relation for friction (Eq. (2*a*). According to Linker and Dieterich [17], for Westerly granite $f_{ss} = 0.7$ and $\alpha = 0.2$, meaning that roughly 30% of the pressure dependence results from the delayed response, with the other 70% being immediate.

Normal stress effects observed by Prakash [19] were also modeled by a modification of the standard rate and state equations. Rather than a two-stage response to normal stress, there is a single prolonged effect. Motivated by Bowden and Tabor [14], e.g., Eq. (3), Prakash [19] decomposed the shear resistance into the product of two functions

$$\tau = f(V,\phi)\psi(\sigma) \tag{6}$$

where ϕ and ψ and are state variables, f is the frictional resistance that depends on slip speed, ϕ is dimensionless, and ψ has the dimensions of stress. The analogy with Eq. (3) is that the contact area (A in Eq. (3)) is a function of normal stress and, thus, is represented by ψ in Eq. (6). Prakash [19] further stipulated that f is given by the standard rate and state equation for friction (2*a*) with Ruina's [25] slip state variable

$$\frac{d\varphi}{dt} = -\frac{V}{d_c}\left[\varphi + ln\left(\frac{V}{d_c}\right)\right] \tag{7}$$

Motivated by the experimental observations in which the response to a normal stress change is an approximately exponential change in shear resistance with slip, Prakash [19] chose a function that is exponential in slip and has a steady state value of σ

$$\frac{d\psi}{dt} = -\frac{V}{d_c}(\psi - \sigma) \tag{8}$$

Prakash [19] allowed for two state variables of the form (8), each with its own characteristic displacement, making a total of three state variables (Eq. (7) and two Eq. (8)s), and three characteristic lengths. To simplify our simulations we have used a single state variable (8) associated with the normal stress response, making a total of two state variables (Eqs. (7) and (8)). Furthermore, we have used a single characteristic length. Following Dieterich [22] and Linker and Dieterich [17], d_c has the interpretation of the representative asperity contact dimension.

Forward simulations based on the formulations of Linker and Dieterich [17], using Eqs. (2*a*) and (2*b*), and Prakash [19], using Eqs. (2*a*), (6), (7) and (8), were done numerically with a Runge-Kutta scheme (Press et al [26]). The machine interaction with the fault is represented using a single degree of freedom slider block model (Eq. (1)). In the experiments the normal stress changes are not strictly abrupt. In the simulations we represent the change in normal stress as an exponential function

$$\sigma = \sigma_0 + \Delta\sigma\left[1 - \exp\left(\frac{-(t-t_0)}{t_c}\right)\right] \tag{9}$$

where t_0 is the time the normal stress change $\Delta\sigma$ is initiated, σ_0 is the initial normal stress, and t_c is the characteristic duration of the change. In the simulations $t_c = 0.02$ s, which matches the duration of the imposed changes well. Note that in the observations (Fig. 4) and in Eq. (9) the duration of the normal stress change is approximately constant while the rate of the change in normal stress decreases as the amplitude of the change decreases.

Figures 5 and 6 illustrate the differences between predictions using the formulations proposed by Linker and Dieterich [17] and those of Prakash [19]. The Linker and Dieterich [17] equations produce an abrupt increase in the state variable as the normal stress is increased. This results in an abrupt increase in strength, therefore, the slip speed decreases. In response, the shear stress increases in load point displacement along a linear loading trend (Fig. 5) with slope kV_L, as expected from Eq. (1) when $V_L \gg V$, where V_L is the load point velocity. In particular, all of the simulated normal stress steps, regardless of size, start out on the same linear trend. The linear increase is followed by a subsequent exponential rise in shear strength to its new steady-state value. Simulations using the formulations of Prakash [19] (Fig. 6) show, on the other contrary, a gradual evolution of the shear strength of the sliding surface in response to a step increase in the normal stress. In the Prakash [19] formulation, the state variable ψ and hence,

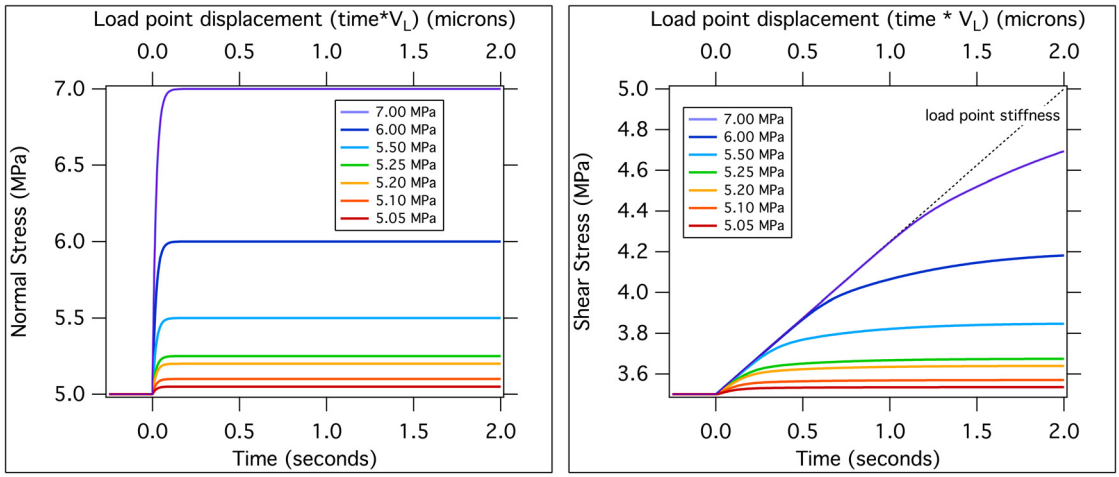

Fig. 5 Forward model of the relations, Eqs. (2*a*) and (2*b*) developed by Linker and Dieterich [19], to simulate their experimental observations. Parameters used in these simulations of our experiments are f_0=0.7, a = 0.008, b = 0.01, d_c= 0.5 μm, α = 0.2 and k = 0.75 MPa/μm. Note the linear rise in shear stress in response to the step change in the applied normal stress. In the shear stress plot is line with slope equal to the estimated stiffness of the loading system (~0.75 MPa/μm) is shown for reference.

the fault strength, changes with fault slip, rather than immediately. Clearly, our new data, at least qualitatively, suggest that the constitutive formulation described by Prakash [19] better describes the evolution of shear strength on a fault in response to sudden changes in the normal stress.

Our observations of the immediate response of the fault closure and contact area (as implied by acoustic amplitude) to changes in normal stress (Fig. 4(*c*)), combined with the gradual changes in the shear strength of the fault, provide unexpected constraints on friction micromechanics. The observations of an immediate increase in the area of contact are consistent with either an elastic component of the contact area increase or a rapid inelastic yielding (Bowden and Tabor [14]), and reinforces the relationship between the total area of contact between two roughened surfaces and the material properties of those surfaces. The relationship between the observed rapid fault closure and the application of a normal load is also consistent with elasticity or abrupt inelastic yielding at asperity contacts in response to the applied load and, accordingly, as the contacts deform under a higher normal load, the fault surfaces move closer together.

Previous work by Hong and Marone [18] shows results that are very similar to Linker and Dieterich [17]. Both studies show the shear stress on a fault responding to changes in the normal stress on that fault at load point displacement rates apparently coincident with the load-point stiffness of the sample assembly used in each test. In the case of Linker and Dieterich [17], where bare granite surfaces were studied, the scale of the plots makes it difficult to accurately distinguish between the loading slope of the instrument/sample assembly and the loading curve for the shear stress of the fault. With the benefit of digital data, while reproducing those experiments, we are able to clearly distinguish between the loading slope of the sample assembly, and the distinctly lower, apparently nonlinear loading slope of the shear stress responding to changes in the normal stress on the fault.

Hong and Marone [18] focus on the response of the shear strength of a fault filled with a layer of gouge in their experiments.

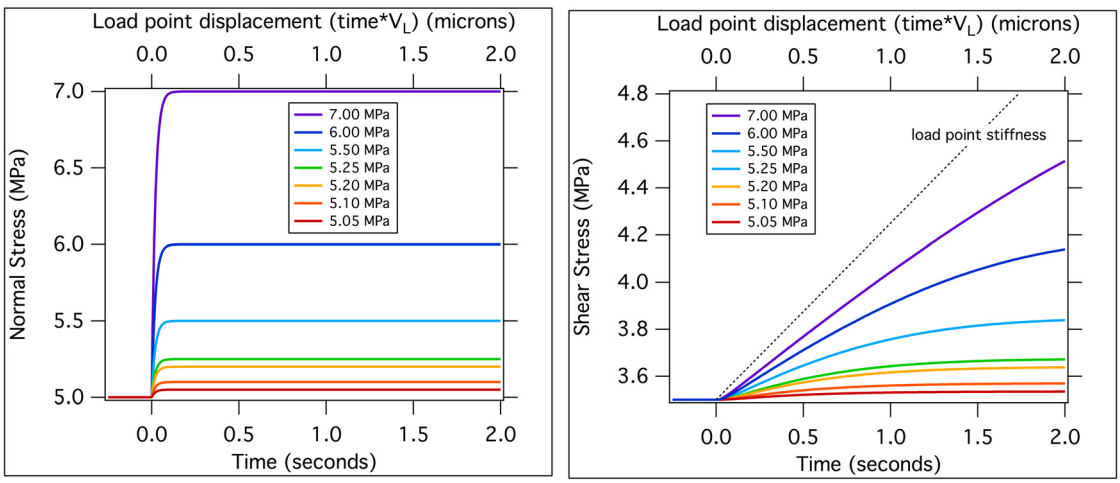

Fig. 6 Forward models of the relations (2*a*), (7), and (8) developed by Prakash [19] to simulate his experimental observations. Parameters used in the simulations of our observations and testing procedure are the same as in Fig. 5: f_0 = 0.7, a = 0.008, b = 0.01, d_c= 0.5 μm, and k = 0.75 MPa/μm. Note the gradual nonlinear rise in shear stress in response to the step change in the applied normal stress. In the shear stress plot a line with slope equal to the estimated stiffness of the loading system (~0.75 MPa/μm) is shown for reference.

Their data plots (e.g., their Fig. 3) show the shear strength of the fault loading coincident with the load-point stiffness of the sample assembly, and are consistent with the two-stage evolution of shear stress proposed by Linker and Dieterich [17]; linear elastic loading, followed by the displacement dependent, roughly exponential, evolution of shear stress to a new steady-state level. However, there are scale differences of more than 200 times which make a direct comparison between their published results and our study difficult. In addition, the results of their simulations (their Fig. 11) show steeper loading slopes relative to the data, which is more consistent with our interpretation rather than Linker and Dieterich's [17]. Therefore, while it appears that our work resolves the discrepancy of previous work regarding the response of the shear strength of an initially bare surface fault to changes in the normal stress, at present our interpretation should not be applied to simulated fault gouge. A more detailed examination of the response of fault gouges to changes in normal stress would better address the differences between our results on initially bare rock surfaces and those of Hong and Marone [18] on simulated gouge layers.

An explanation for the gradual rise in shear strength is not immediately apparent, either from classic or rate and state theories of friction. The adhesion or plastic junction model of Bowden and Tabor [14], Eqs. (3) or (6), which provides the basis of Prakash's [19] interpretation, equates the shear strength of an interface to the product of area of contact and the material yield strength of contacts. In Prakash's [19] implementation, he attributes the evolution of shear strength as normal stress changes as being due to increasing contact area with slip (his state variable, designated here as Ψ with evolution prescribed by Eq. (8)). While this kind of slip- or time-dependent yielding may be expected for many materials, particularly for metals, as in Bowden and Tabor [14], our experimental observations from acoustic transmission imply an immediate increase in the contact area with increasing normal stress, precluding Prakash's [19] physical interpretation. At the same time, the immediately increasing contact area, while consistent with the interpretation of Linker and Dieterich [17], apparently does not lead to an immediate increase in the shear strength of the sliding surface. That is, our observations require that the immediately created contact area lacks shear strength.

For a qualitative interpretation of our new results, we propose that any new contact area that appears as a result of a step increase in normal stress appears with no inherent shear strength. Any new area of contact should assume an area consistent with the yield strength of the material and the applied normal load. However, with no time with which to strengthen, nor any slip with which to develop any shear traction, this new area of contact does not appear to contribute to the shear resistance of the fault. Within the framework of rate- and state-friction, we assert that state, representing the age and shear strength of contact area averaged over the entire sample, drops abruptly due to the addition of the new contact area, which appears with a value of state close to or equal to zero. As slip proceeds, the value of state for the new surface (old + new contacts) evolves back to its prior steady-state value, as the contact area strengthens as a function of elapsed time and the accumulation of shear traction. Our observations are consistent with the assertion of Linker and Dieterich [17] that as normal stress is abruptly raised, state abruptly drops, however, our definition of state differs.

For steps down in normal stress, Linker and Dieterich [17] assume that state (effective contact time) behaves symmetrically with respect to steps up in normal stress; at the instant normal stress drops, state instantly rises, and then evolves back to its prior steady-state level as slip accumulates. Results from this study would suggest that the behavior of state, and possibly the definition of state, might not be so straightforward. We would predict that as the normal stress is dropped, the area of contact is simultaneously lost according to the yield strength of the material. However, based on the results of this study, the shear strength of that lost area of contact could be difficult to estimate. It may also be reasonable to speculate that the surviving area of contact immediately following a step down in normal stress, should have an apparent age that is much older, relative to the contact area that will be created on the fault at the new lower shear and normal stresses. However, how the apparent age of the surviving area of contact interacts with the unknown shear strength of surviving contacts renders predictions of the behavior of state associated with down steps in normal stress uncertain at this time.

A micro-mechanical model of these observations notwithstanding, our results have implications for how complex fault geometries affect fault rupture propagation, and for how improved earthquake simulations should incorporate normal stress sensitivity. Though the implications of our results are unexplored in dynamic rupture models, qualitatively we expect differences from the predictions of Linker and Dieterich [17]. In regions of increasing stress (both normal and shear stress), Linker and Dieterich's [17] observations would suggest immediately increasing shear resistance, and little acceleration of fault slip. In contrast, our data suggest no immediate change in shear resistance; thus, an increasing slip rate would be expected. The converse would be true in regions of decreasing shear and normal stress. Ultimately, our lab observations can be incorporated to improve earthquake hazard mitigation efforts. For example, earthquakes in the 2007 uniform California earthquake rupture forecast (UCERF2) are based on segmented faults, where earthquakes can only rupture a single segment. Relaxing rigid segmentation and allowing multi-fault ruptures are key enhancements under development for the next generation rupture forecast. In order to implement these changes to the forecast, the effects of complex fault geometries, including fault step-overs, nonplanar faulting, and multi-fault intersections, will need to be incorporated into the model. This will require detailed knowledge of how shear strength changes with fault normal stress.

5 Conclusions

The results of the current study show that the shear strength of an initially bare surface fault gradually evolves after a sudden increase in the normal stress applied to that fault. While friction on bare surface faults appears to evolve relatively slowly following a step increase in the normal stress, the gap between the fault surfaces, and the apparent area of contact between the fault surfaces, inferred from acoustic transmission data, appear to respond immediately. Numerical implementation of the model proposed by Prakash [19] appears to simulate our data better than the model proposed by Linker and Dieterich [17]. However, the physical basis for the model proposed by Prakash [19], in which contact area changes slowly in response to changes in normal stress ,is not consistent with our acoustic transmission data.

Finally, these new results have implications for fault strength during static and dynamic stress transfer at fault junctions, the interactions of multiple faults in complex structural settings, and for dynamic fault rupture as slip propagates through or terminates at such complex fault geometries. If fault strength does not evolve immediately with normal stress increments, then the unstable response of faults to unclamping and the stable response to clamping may be minimized. In turn, these results could have implications for the ability of ruptures to propagate across geometrical boundaries in fault systems, where rapid changes in normal stress are expected.

Acknowledgment

We would like to thank Jim Dieterich for insightful discussion, and Kohei Nagata for technical guidance and helpful discussions related to this work. Kohei conducted normal stress step experiments on Lucite plastic and granite, which are the basis of the present study. Insightful reviews by Diane Moore, Carolyn Morrow, and one anonymous reviewer substantially improved this paper. This research was supported by the U.S. Geological Survey and by

the Southern California Earthquake Center through a research grant to the University of California at Riverside. The SCEC is funded by the NSF Cooperative Agreement No. EAR-0106924 and the USGS Cooperative Agreement No. 02HQAG0008. The SCEC contribution number for this paper is 1516.

References

[1] Harris, R. A., Archuleta, R. J., and Day, S. M., 1991, "Fault Steps and the Dynamic Rupture Process—2-D Numerical Simulations of a Spontaneously Propagating Shear Fracture," Geophys. Res. Lett., **18**(5), pp. 893–896.

[2] Andrews, D. J., and Ben-Zion, Y., 1997, "Wrinkle-Like Slip Pulse on a Fault Between Different Materials," J. Geophys. Res., **102**(1), pp. 552–571.

[3] Bouchon, M., and Streiff, D., 1997, "Propagation of a Shear Crack on a Nonplanar Fault: A Method of Calculation," Bull. Seismol. Soc. Am., **87**(1), pp. 61–66.

[4] Harris, R. A., and Day, S. M., 1997, "Effects of a Low-Velocity Zone on a Dynamic Rupture," Bull. Seismol. Soc. Am., **87**(5), pp. 1267–1280.

[5] Harris, R. A., and Day, S. M., 1993, "Dynamics of Fault Interaction—Parallel Strike-Slip Faults," J. Geophys. Res., **98**(B3), pp. 4461–4472.

[6] Kame, N., Rice, J. R., and Dmowska, R., 2003, "Effects of Pre-Stress State and Rupture Velocity on Dynamic Fault Branching," J. Geophys.Res., **108**(B5), p. 2265.

[7] Bhat, H. S., Dmowska, R., Rice, J. R., and Kame, N., 2004, "Dynamic Slip Transfer from the Denali to Totschunda Faults, Alaska: Testing Theory for Fault Branching," Bull. Seismol. Soc. Am., **94**, pp. S202–S213.

[8] Duan, B., and Oglesby, D. D., 2005, "Multicycle Dynamics of Nonplanar Strike-Slip Faults," J. Geophys. Res., **110**, p. B03304.

[9] Oglesby, D. D., 2005, "The Dynamics of Strike-Slip Step-Overs With Linking Dip-Slip Faults," Bull. Seismol. Soc. Am., 95(5), pp. 1604–1622.

[10] Wesnousky, S. G., 2006, "Predicting the Endpoints of Earthquake Ruptures," Nature (London), **444**, pp. 358–360.

[11] Wesnousky, S. G., 2008, "Displacement and Geometrical Characteristics of Earthquake Surface Ruptures: Issues and Implications for Seismic-Hazard Analysis and the Process of Earthquake Rupture," Bull. Seismol. Soc.Am., **98**(4), pp. 1609–1632.

[12] Weertman, J., 1980, "Unstable Slippage Across a Fault that Separates Elastic Media of Different Elastic Constants," J. Geophys. Res., **85**, pp. 1455–1461.

[13] Harris, R. A., and Day, S. M., 2005, "Material Contrast Does Not Predict Earthquake Rupture Propagation Direction," Geophys. Res. Lett., **32**, p. L23301.

[14] Bowden, F. P., and Tabor, D., 1950, *The Friction and Lubrication of Solids*, Oxford University Press, New York..

[15] Hobbs, B. E., and Brady, B. H. G., 1985, "Normal Stress Changes and the Constitutive Law for Rock Friction (Abstract)," EOS Trans. Am. Geophys.Union, **66**, pp. 382.

[16] Olsson, W. A., 1988, "The Effects of Normal Stress History on Rock Friction, Key Questions in Rock Mechanics," *Proceedings of the 29th U.S. Symposium on Rock Mechanics*, P. A. Cundall, R. L. Sterling, and A. M. Starfield, eds., University of Minnesota, June 13–15, A.A. Balkema, Rotterdam, pp. 111–117.

[17] Linker, M. F., and Dieterich, J. H., 1992, "Effects of Variable Normal Stress on Rock Friction: Observations and Constitutive Equations," J. Geophys. Res., **97**, pp. 4923–4940.

[18] Hong, T., and Marone, C., 2005, "Effects of Normal Stress Perturbations on the Frictional Properties of Simulated Faults," Geochem. Geophys. Geosyst., **6**, p. Q03012.

[19] Prakash, V., 1998, "Frictional Response of Sliding Interfaces Subjected to Time Varying Normal Pressures," ASME J. Tribol., **120**, pp. 97–102.

[20] Ranjith, K., and Rice, J. R., 2001, "Slip Dynamics at an Interface Between Dissimilar Materials," J. Mech. Phys. Solids, **49**, pp. 341–361.

[21] Rice, J. R., Lapusta, N., and Ranjith, K., 2001, "Rate and State Dependent Friction and the Stability of Sliding Between Elastically Deformable Solids," J. Mech. Phys. Solids, **49**, pp. 1865–1898.

[22] Dieterich, J. H., 1978, "Time-Dependent Friction and the Mechanics of Stick Slip," Pure Appl. Geophys., **116**, pp. 790–806.

[23] Nagata, K., Nakatani, M., and Yoshida, S., 2008, "Monitoring Frictional Strength With Acoustic Wave Transmission," Geophys. Res. Lett., **35**, L06310.

[24] Nagata, K., Kilgore, B., Beeler, N. M., and Nakatani, M., 2010, "Simultaneous Measurement of Real Contact Area and Fault Normal Stiffness During Frictional Sliding," Abstract T33A-2220, presented at 2010 Fall Meeting, American Geophysical Union, 13–17 Dec., San Francisco, CA.

[25] Ruina, A. L., 1983, "Slip Instability and State Variable Friction Laws," J. Geophys. Res., **88**, pp. 10359–10370.

[26] Press, W. H., Flannery, B. P., Teukolsky S. A., and Vetterling, W. T., 1986, *Numerical Recipes: The Art of Scientific Computing*, Cambridge University Press, Cambridge.